



# Trimming laser-written waveguides through overwriting

THOMAS WILL,<sup>1,2,4</sup> JUN GUAN,<sup>3,5</sup> PATRICK S. SALTER,<sup>3</sup>  AND MARTIN J. BOOTH<sup>2,3,6</sup> 

<sup>1</sup>*Institute of Photonic Technologies, Friedrich-Alexander University Erlangen-Nürnberg, Konrad-Zuse-Straße 3/5, 91052 Erlangen, Germany*

<sup>2</sup>*Erlangen Graduate School in Advanced Optical Technologies (SAOT), Friedrich-Alexander University Erlangen-Nürnberg, Germany*

<sup>3</sup>*Department of Engineering Science, University of Oxford, Parks Road, Oxford OX1 3PJ, UK*

<sup>4</sup>*thomas.will@fau.de*

<sup>5</sup>*jun.guan@eng.ox.ac.uk*

<sup>6</sup>*martin.booth@eng.ox.ac.uk*

**Abstract:** Femtosecond laser direct writing is widely used to create waveguide circuits for optical processing in applications including communications, astrophotonics, simulation and quantum information processing. The properties of these waveguide circuits can be sensitive to the fabrication conditions, meaning that noticeable variability can be present in nominally identical manufactured components. One potential solution to this problem is the use of device trimming, whereby additional laser fabrication is applied to optimise the optical properties of a device based upon measurement feedback. We show how this approach can be used in the manufacture of directional couplers by overwriting the laser-written structure to alter the coupling ratios.

Published by The Optical Society under the terms of the [Creative Commons Attribution 4.0 License](https://creativecommons.org/licenses/by/4.0/). Further distribution of this work must maintain attribution to the author(s) and the published article's title, journal citation, and DOI.

## 1. Introduction

Integrated optical circuits are used for the control and processing of optical signals in a range of applications including tunable lasers [1], transmitters [2] and integrated receivers [3]. There have been many advances in the miniaturization of these circuits to enable complex on-chip designs. One core building block is the directional coupler (DC) which operates as a waveguide based beam splitter. In a directional coupler, two waveguides are closely spaced so that the evanescent fields of the waveguides overlap and therefore can exchange energy [4–8].

The femtosecond laser direct-write (FLDW) technique is commonly used to fabricate waveguides in glass substrates [9]. The FLDW technique uses a tightly focused femtosecond pulsed laser to achieve high intensity in a confined focal volume, which results in nonlinear optical effects. Depending on the material processed, the laser writing can cause a positive refractive index change, thus producing three dimensional waveguides by translating the substrate with respect to the focus [10,11].

Many applications ranging from electro-optical modulators [12] to quantum logic gates [5,13,14] and boson sampling [5,15,16] benefit from the usage of FLDW beam splitters. For optimal performance of the waveguide circuits, the two outputs of the DC should have designed splitting ratios and phase differences between each other, for which a precisely controllable and highly repeatable fabrication process is required [14]. Performance and repeatability of the writing process is improved through modelling and process optimisation, although there are often variations between seemingly identical waveguides due to minor fluctuations in the laser power or mechanical effects between waveguides [17,18,19]. This in turn makes it necessary to

perform extensive parameter studies of DCs to determine the needed geometric parameters and the optimal laser characteristics (e.g. pulse energy and repetition frequency) for fabricating a DC with a specific splitting ratio and phase difference [13].

A defined change in the optical path length of one of the waveguides of the DC allows for a controlled change of the splitting ratio and therefore gives the possibility to improve the repeatability in fabricating DCs. In principle, a change of the optical path length of a waveguide is possible by adjusting its refractive index. This may be implemented through an external stimulus to the glass surface to induce thermo-optical [20] or strain-optic [21] adaptive tuning of the refractive index and achieve specified output ratios. However, this approach is only applicable to near-surface waveguides and thus not suitable for complex three-dimensional waveguide structures. Alternatively, tuning may be achieved with the FLDW fabrication method itself, either through the introduction of additional stresses in the glass [17] or by overwriting one of the waveguides, which allows modification of its refractive index [22] and therefore the splitting ratio and phase difference of a DC [23].

In this report, we first demonstrate the influence of overwriting on the mode shape of waveguide structures which is correlated to a change in refractive index. Secondly, we present a proof-of-principle demonstration of changing the splitting ratio by overwriting specific geometric sections of a DC.

## 2. Theory and simulation

A geometrically symmetrical DC fabricated using FLDW consists of two waveguides and can be subdivided into a straight section, S-bend section and straight interaction region. In order to achieve a defined power transfer, it is essential to know values of the variables influencing the splitting ratio. For the derivation of energy coupling between waveguides, the theory of coupled modes (CMT) is used [6,7]. Assuming that light is only coupled into one waveguide ( $w_1$ ), the specific power splitting ratio  $\alpha$  of a DC can be defined with the help of CMT [24] as followed

$$\alpha = \frac{P_2}{P_1 + P_2} = \sigma^2 \cdot \sin^2 \left( \frac{\kappa}{\sigma} \cdot L_0 + \phi \right) \quad (1)$$

and corresponds to the normalized power coupled into waveguide  $w_2$ . Here,  $P_1$  is the optical power of the transmitted light at the output port of waveguide  $w_1$  and  $P_2$  is the optical power of the coupled light at the output port of waveguide  $w_2$ . The coupling coefficient  $\kappa$  characterises the interaction of the waveguides and is proportional to the overlap integral of the exponentially decaying evanescent field [8]. This coefficient depends on the channel width, the separation distance of the waveguides, the wavelength and the polarization direction of the coupled light [6]. A contribution of the bent waveguide regions to the splitting ratio of the DC can be found, which is expressed by a bending phase term  $\phi$ . For a DC with a fixed geometry and interaction length  $L_0$ , the power splitting ratio changes when a phase mismatch is applied by altering the amplitude dephasing term  $\sigma$  [24]:

$$\sigma = 1 / \sqrt{1 + \left( \frac{\Delta\beta}{2\kappa} \right)^2} \quad (2)$$

with asymmetry related to the difference in the propagation constants  $\Delta\beta$  for the two arms of the DC:

$$\Delta\beta = |\beta_1 - \beta_2| = \frac{2\pi\Delta n}{\lambda_o} \quad (3)$$

In consequence of an increasing asymmetry, the maximum power coupling ratio  $\sigma^2$  decreases from unity to fractional values, and a refractive index change  $\Delta n$  in one of the waveguides of a DC can be used to modulate the splitting ratio.

Simulations were performed to describe the influence of overwriting specific parts of a DC and their subsequent influence on the splitting ratio (COMSOL Multiphysics version 5.3). The cladding material was defined with a refractive index  $n_{eff} = 1.50$ , which is approximately the value for the refractive index of borosilicate glass (Corning Eagle2000) at a wavelength at  $\lambda_0 = 785$  nm. The waveguide itself was defined with a higher refractive index  $n_{core} = 1.503$ . Overwriting was modelled for one of the waveguides in the DC by assuming an increase of the waveguide core refractive index for either the entire length, or just the interaction region, the S-bend section or the straight section at the start and end of the DC. The refractive index change  $dn_{OW}$  was varied in steps of  $1 \times 10^{-4}$ , following previous work in Ref. [22] on overwriting waveguides with a MHz pulse repetition rate laser source. The interaction length  $L_0$  was changed from 1.50 mm up to 6.50 mm with 0.10 mm-steps each to probe the sinusoidal response of Eq. (1). The splitting ratio was finally calculated by integrating the electric field of each output port of the simulated DC.

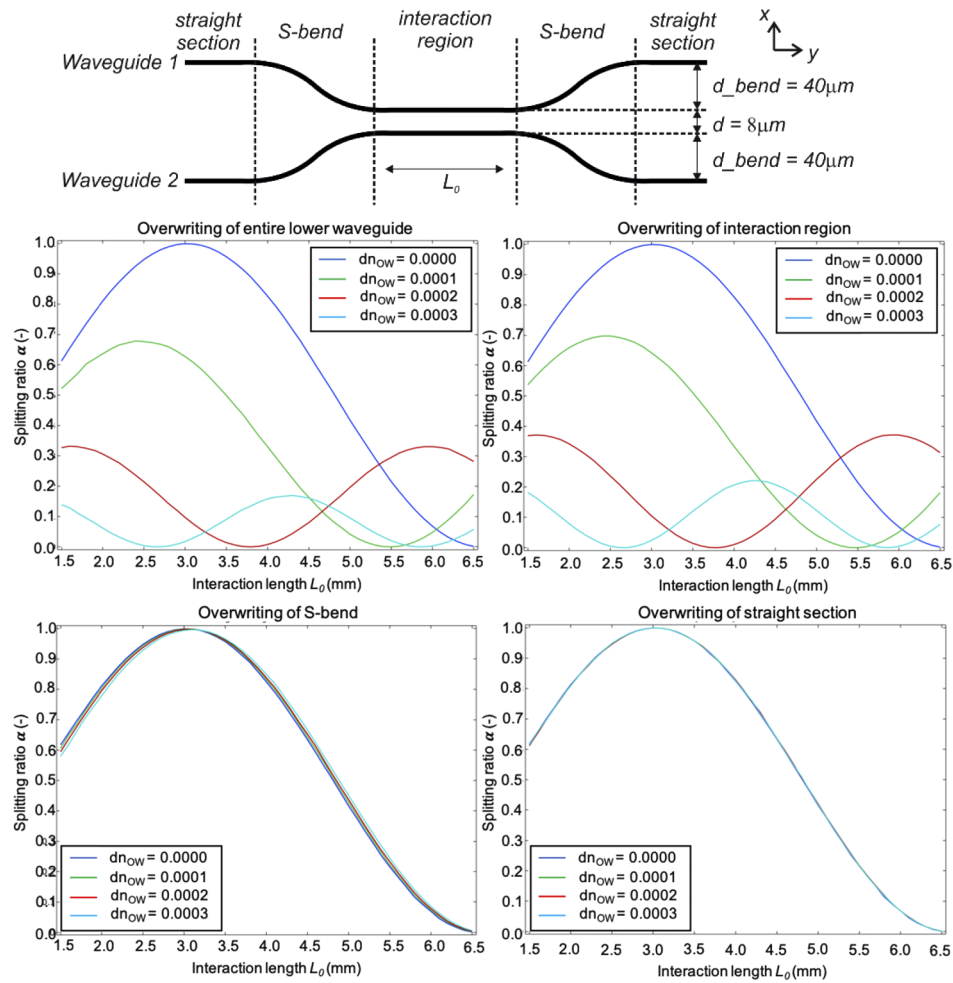


**Fig. 1.** Schematic design for the directional coupler (top). Simulation results for splitting ratio  $\alpha$  over interaction length  $L_0$  for overwriting the entire length of waveguide 2 (upper left), just the interaction region (upper right), just the S-bend (bottom left) or just the straight section (bottom right). Overwriting is simulated by an increase of refractive index by  $dn_{OW} = 0.0000$  up to  $dn_{OW} = 0.0003$ .

The simulation results in Fig. 1 show that an increase of the refractive index decreases the amplitude of the sinusoidal response  $\sigma^2$  from unity to non-linearly decreasing fractional values for overwriting the entire length of waveguide 2 ( $\sigma^2 = 0.679$  for  $dn_{OW} = 0.0001$ ,  $\sigma^2 = 0.330$  for  $dn_{OW} = 0.0002$  and  $\sigma^2 = 0.170$  for  $dn_{OW} = 0.0003$ ) or the interaction region ( $\sigma^2 = 0.698$  for  $dn_{OW} = 0.0001$ ,  $\sigma^2 = 0.372$  for  $dn_{OW} = 0.0002$  and  $\sigma^2 = 0.221$  for  $dn_{OW} = 0.0003$ ). There is an associated phase shift in the sinusoidal response with the peak in the splitting ratio occurring at a different interaction length  $L_0$ . We note that an equivalent refractive index change has a greater effect on the amplitude of the sinusoidal response of the splitting ratio when overwriting the entire lower waveguide as opposed to just the interaction region. This result is due to the fact that the total induced phase mismatch is slightly larger as the increased refractive index of the S-bend also influences the propagation constants.

Overwriting of just the straight waveguide sections at the start and end of the DC is found to have no effect on the splitting ratio, as expected. Meanwhile, overwriting of the S-bend has a slight influence on the splitting ratio by inducing a shift in the sinusoidal splitting-ratio function. Nevertheless, the influence of the S-bend is rather negligible for low refractive index increases ( $dn_{OW} = 0.0001$ ) and becomes more relevant at higher refractive index increases ( $dn_{OW} = 0.0003$ ). In consequence, to avoid the influence of the S-bend structure, the overwriting of the interaction region seems to be sufficient and allows easier adjustment of the splitting ratio.

### 3. Experimental methods

Waveguide writing was performed using a frequency-doubled regeneratively amplified Yb:KGW laser (Light Conversion Pharos SP-06-1000-pp) with a pulse duration of 168 fs, a wavelength of 514 nm and a maximum average power of up to 6 W. The pulse repetition frequency was set to 1 MHz. The average laser power was adjusted by a combination of a motorised rotating half-wave plate and a polarization beam splitter. In this study, the laser power was set to an average power of 91 mW, which was measured before the glass specimen. The beam was first expanded and then phase-modulated by a liquid-crystal on silicon spatial light modulator (SLM) (Hamamatsu Photonics X10468-09(X)) to correct system aberrations and depth dependent spherical aberration at certain writing depths [25]. Afterwards, the SLM was imaged in a 4-f system onto the pupil plane of a microscope objective 0.50 NA (20 $\times$ ; Zeiss Plan Neofluar). Finally, the modulated beam was focused inside a borosilicate glass specimen (Corning Eagle2000) (20  $\times$  20  $\times$  1.15 mm<sup>3</sup>) at a depth of 170  $\mu$ m. The specimen was mounted on a three-axis air bearing translation stage (Aerotech ABL10100L, xy-motion; ANT95-3-V, z-motion) and was moved transverse to the linearly polarized laser beam with waveguide axis along the y direction and laser polarization along the x direction. After the waveguide fabrication, the post-processing of the specimen consisted of polishing the two end-facets of the glass chip to receive a cross-sectional view at the input and output ports of the waveguides.

Two types of waveguide structures were written. First, straight waveguides were written with different writing speeds from 12.5 mm/s to 17.5 mm/s and different overwriting repetitions to investigate associated changes in the shape of the transmitted mode. Secondly, directional couplers were written for the investigation of the splitting ratio with a constant writing speed of 17.5 mm/s and overwriting different sections of one waveguide arm  $w_2$ . Overwriting was performed by repeating the writing process with the same writing parameters. The overwriting repetitions and the scanning speed were varied in order to determine the optimum writing parameters. We combine these parameters into the representative net fluence (*RNF*). Similar to the definition of net fluence in Ref. [26,27], here the writing *RNF* is defined as:

$$RNF = \frac{4R_f E_p (OW + 1)}{\pi v_w D}, \quad (4)$$

where  $R_f$  is the pulse repetition rate,  $E_p$  is the pulse energy measured at sample surface,  $OW$  is the number of overwriting repetitions and  $v_w$  is the scanning speed of the translation stage.  $D$  is the focal spot diameter, approximated as  $D = 1.03 \mu\text{m}$  as the ratio of the wavelength and the numerical aperture of the microscope objective for the writing laser.

The schematic DC geometry can be found in Fig. 1 and is consistent with that used in the simulations of Section 2. The S-bend was formed by two circle sections with a radius of curvature  $R = 40 \text{ mm}$ . The radius of curvature of the S-bend  $R = 40 \text{ mm}$  was chosen to reduce bend losses [18]. The displacement along the x-axis was set to be  $d_{\text{bend}} = 40 \mu\text{m}$  to allow a sufficient distance between the input and output straight sections to avoid energy exchange. The interaction region  $L_0$  was variable to probe the sinusoidal behaviour of the power splitting function. The centre-to-centre separation at the interaction region was set to  $d = 8 \mu\text{m}$  to space the waveguides sufficiently close for energy exchange [18].

The mode field diameter (MFD) of the fabricated waveguides was measured with a butt-coupled rig. Here a polarization-maintaining single-mode fibre (Thorlabs PM630-HP (PANDA)) was directly butted in contact with a waveguide in order to couple light of wavelength 785 nm (Thorlabs S1FC780PM). The near field mode profile was measured by imaging the intensity profile of the light transmitted from a waveguide output port with the help of an ultra-long working distance microscope objective (Olympus ULWD 80 $\times$  0.75NA MS Plan, dry) onto a CCD camera (Baumer TXD-14).

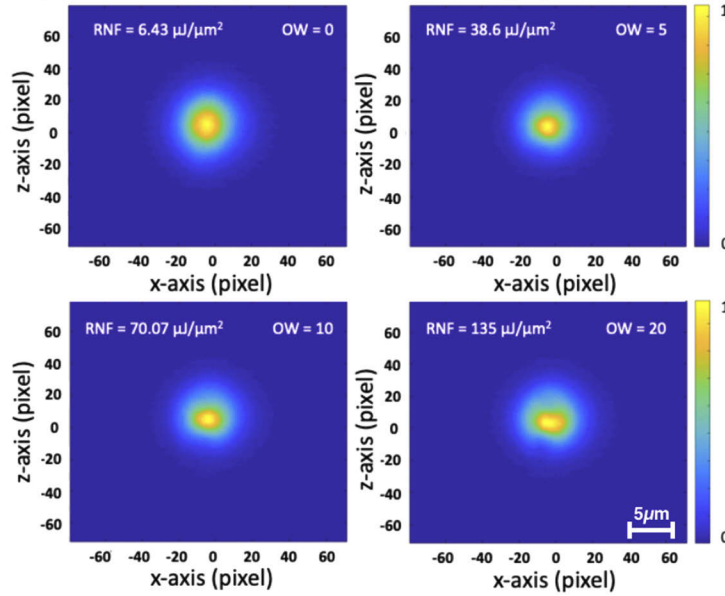
The splitting ratio of directional couplers was determined with free-space coupling of a diode laser beam at 785 nm, which was focused with a lens onto the input port of a DC to couple light into one of the waveguides. The splitting ratio was measured by imaging the output ports of the DC with a camera and integrating the intensity of the images which correspond to the output power. As a consequence, the splitting ratio was determined according to Eq. (1). The free-space coupling was chosen here due to an automated evaluation algorithm [28] which allowed measurement of several DCs within seconds with high repeatability.

### 3.1. Overwriting straight waveguide

The shape of the propagating mode supported by each of the straight waveguides was characterized as a function of the representative net fluence  $RNF$  during writing, remembering that there is a linear increase of the  $RNF$  with each overwriting scan as described in Eq. (4). The results show that the mode shape changes from slightly elliptical to a circular cross-section and the MFD is reduced for increasing  $RNF$  up to  $70.07 \mu\text{J}/\mu\text{m}^2$  (see Fig. 2). For further overwriting repetitions ( $v_w = 17.5 \text{ mm/s}$ ;  $OW = 10$ ;  $RNF = 70.07 \mu\text{J}/\mu\text{m}^2$ ) the mode profile becomes enlarged along the x-axis, while the profile in z-direction (along the laser fabrication beam axis) does not seem to be influenced, with an increasingly elliptical mode shape in consequence. For further overwriting repetitions ( $v_w = 17.5 \text{ mm/s}$ ;  $OW = 20$ ;  $RNF = 135 \mu\text{J}/\mu\text{m}^2$ ), damage of the glass matrix started to occur, and was visible in both microscope images and transmitted mode profiles.

Figure 3 fully quantifies the MFD for the waveguides along the z-axis and x-axis as a function of  $RNF$ . The initial decrease of  $MFD_x$  with  $RNF$  is clearly visible and can be explained as an increase in waveguide refractive index with overwriting, consistent with the results from Ref. [22], which in turn leads to reduced size of the MFD. The increased refractive index is likely due to a stronger modification of the material due to the increased deposited energy with overwriting. Chen et al. [24] investigated the MFD of DCs in borosilicate glass (Corning Eagle2000) and showed that by decreasing the writing speed from  $v_w = 20 \text{ mm/s}$  to  $v_w = 12 \text{ mm/s}$  the MFD shrank from  $11.2 \mu\text{m}$  to  $8.9 \mu\text{m}$ , consistent with the reduction of the MFD at higher fluence observed here. At higher values of the  $RNF$  above  $70 \mu\text{J}/\mu\text{m}^2$ ,  $MFD_x$  starts to rise which might indicate an increased waveguide diameter. Findings show that in the cumulative-pulse regime an increase in the size of the modified structure can be observed in borosilicate glass for increasing number of pulses [29], which is also reasonable for the overwriting conditions described here.



Colour-map of near field mode profile for different overwriting repetitions OW at  $v_w = 17.5$  mm/s

**Fig. 2.** Colour-map images of the near field mode profile is shown with normalized intensity values for different overwriting repetitions  $OW = 0$ ,  $OW = 5$ ,  $OW = 10$  and  $OW = 20$  for one writing speed  $v_w = 17.5$  mm/s. These overwriting repetitions correspond to a net fluence  $RNF$  of  $6.43 \mu\text{J}/\mu\text{m}^2$ ,  $38.6 \mu\text{J}/\mu\text{m}^2$ ,  $70.7 \mu\text{J}/\mu\text{m}^2$  and  $135 \mu\text{J}/\mu\text{m}^2$ . Axis values show the distance in pixels (1 pixel =  $0.18 \mu\text{m}$ ) from the centre of the image. The centre is defined at the point, where maximum intensity can be found.

In comparison to the  $MFD_x$ , the  $MFD_z$  shows slightly different characteristics for increasing  $RNF$ . The  $MFD_z$  shows an initial decrease of the MFD with  $RNF$ , analogous to the  $MFD_x$ , again explained by an increase in refractive index increase. However, the decrease of the  $MFD_z$  is greater than that for  $MFD_x$ , which is possibly related to asymmetry in the focusing created by the existing waveguide structure during the overwrite process. In contrast to  $MFD_x$ , no increase of  $MFD_z$  can be seen for  $RNF$  greater than  $65.0 \mu\text{J}/\mu\text{m}^2$ . This finding might be related to the formation of damage in the waveguide at higher  $RNF$ , which then limits further expansion of the waveguide structure in the  $z$  direction.

As the MFD along  $x$ - and  $z$ -axis show different results, a change in the ellipticity is expected for increasing overwriting repetitions (see Fig. 4). A waveguide can be considered to be circular as soon as the ellipticity  $\varepsilon$  is greater than 0.87 [30], which is indicated as black dotted line in Fig. 4. There is initially a roughly linear increase to circularity for each writing speed as overwriting is performed and the induced fluence increases. This increase in circularity is due to the strongly decreasing  $MFD_z$  in comparison to the slowly decreasing  $MFD_x$  (compare Fig. 3). After reaching a perfectly circular shape the ellipticity  $\varepsilon$  decreases with increasing  $RNF$ , which corresponds to the findings from Fig. 2 where a non-uniform waveguide structure can be seen at  $RNF = 135 \mu\text{J}/\mu\text{m}^2$ . This increasingly elliptical shape for increasing fluence can be accounted for by a relatively constant  $MFD_z$  and strongly increasing  $MFD_x$  for  $RNF$  higher than approximately  $60 \mu\text{J}/\mu\text{m}^2$  (compare Fig. 3). Small differences in ellipticity can be seen in Fig. 4 depending on the writing speed. The maximum circularity of approximately  $\varepsilon = 1$  is shifted towards higher fluences for an increase of the writing speed.

In summary, a change in the MFD of straight waveguides can be induced by controlling the deposited energy during overwriting. Losses are expected to decrease significantly with

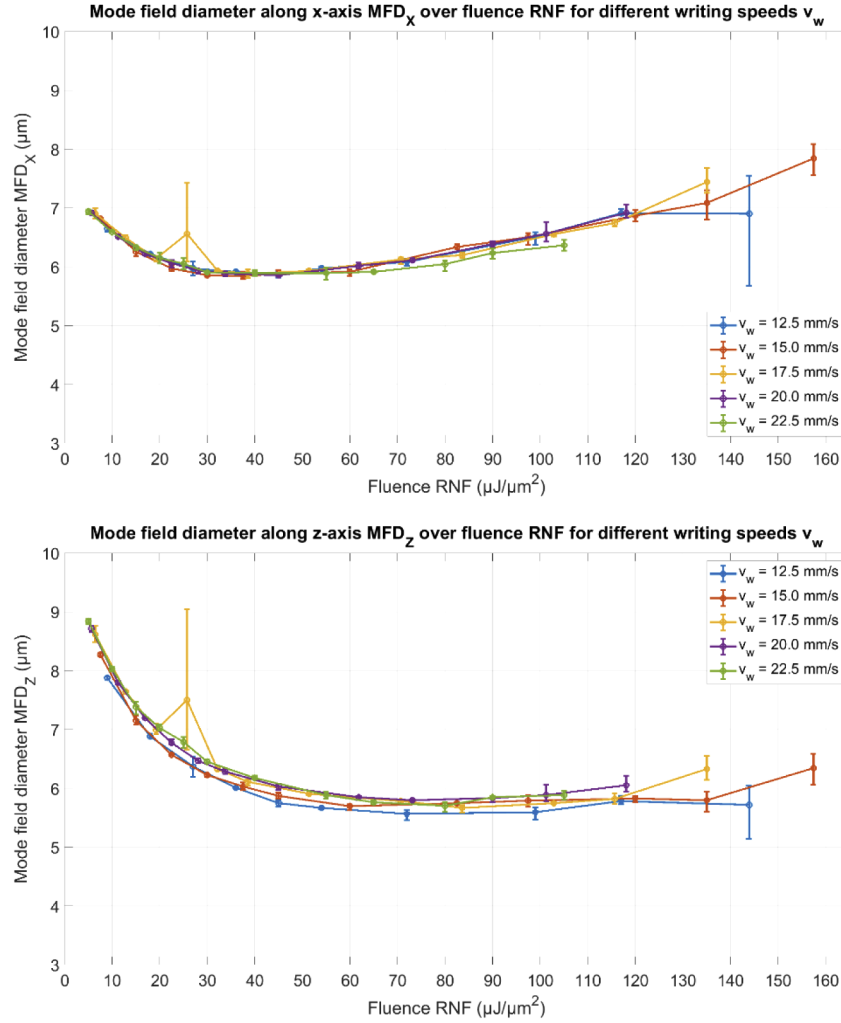


**Fig. 3.** MFD along the x-axis  $MFD_x$  (above) and along the z-axis  $MFD_z$  (below) for different overwriting repetitions  $OW$  from  $OW = 0$  to  $OW = 20$  and writing speeds  $v_w = 15.0$  mm/s and  $v_w = 22.5$  mm/s. For  $v_w = 12.5$  mm/s the data points correspond to  $OW$  from  $OW = 0$  to  $OW = 15$ . Values of the overwriting repetitions are transformed into the representative net fluence to make the results comparable. Each point of the RNF along one plot of a writing speed corresponds to an overwriting scan repetition. For each parameter, the maximum MFD and the minimum MFD is shown as a deviation out of three waveguides in one chip. A high deviation can be found at  $RNF = 25.7 \mu\text{J}/\mu\text{m}^2$ . This is due to a damaged chip-facet at one waveguide which is influencing the evaluation. At higher fluence values  $RNF$  increases the deviation as the resulting mode shape cannot be considered a Gaussian mode profile and thus the fit is not accurate enough.

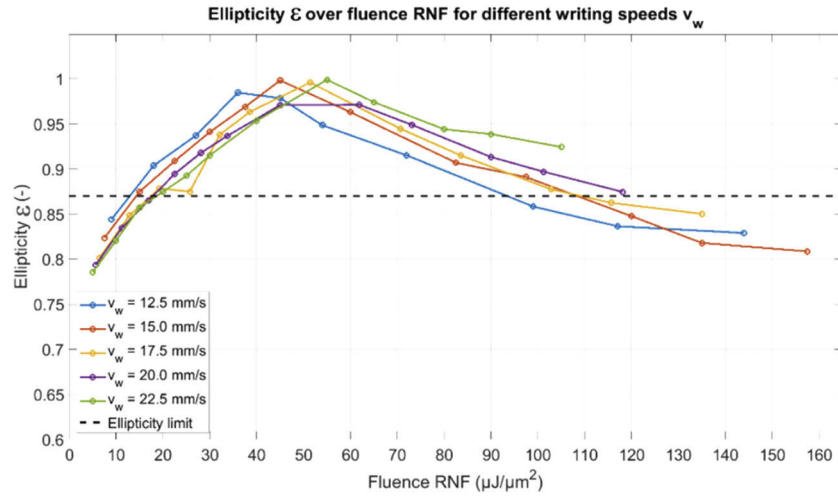


**Fig. 4.** Ellipticity  $\varepsilon$  for different overwriting repetitions  $OW$  from  $OW = 0$  to  $OW = 20$  and writing speeds  $v_w = 15.0$  mm/s and  $v_w = 22.5$  mm/s. For  $v_w = 12.5$  mm/s the data points correspond to  $OW$  from  $OW = 0$  to  $OW = 15$ . Values of the overwriting repetitions are transformed into the resulting net fluence  $RNF$  to make the results comparable. Values correspond to the ellipticity of the averaged parameter points. The black dotted line indicates at which point a circular mode shape is achieved ( $\varepsilon > 0.87$  [30]). Overall error bars are small and hence omitted.

overwriting repetitions [31,32] and approach an asymptote with an increasingly asymmetrical waveguide structure [32]. The change in the MFD is assumed to be related to an increase of refractive index and shows the feasibility of inducing a phase mismatch in a directional coupler by overwriting one arm to control the splitting ratio.

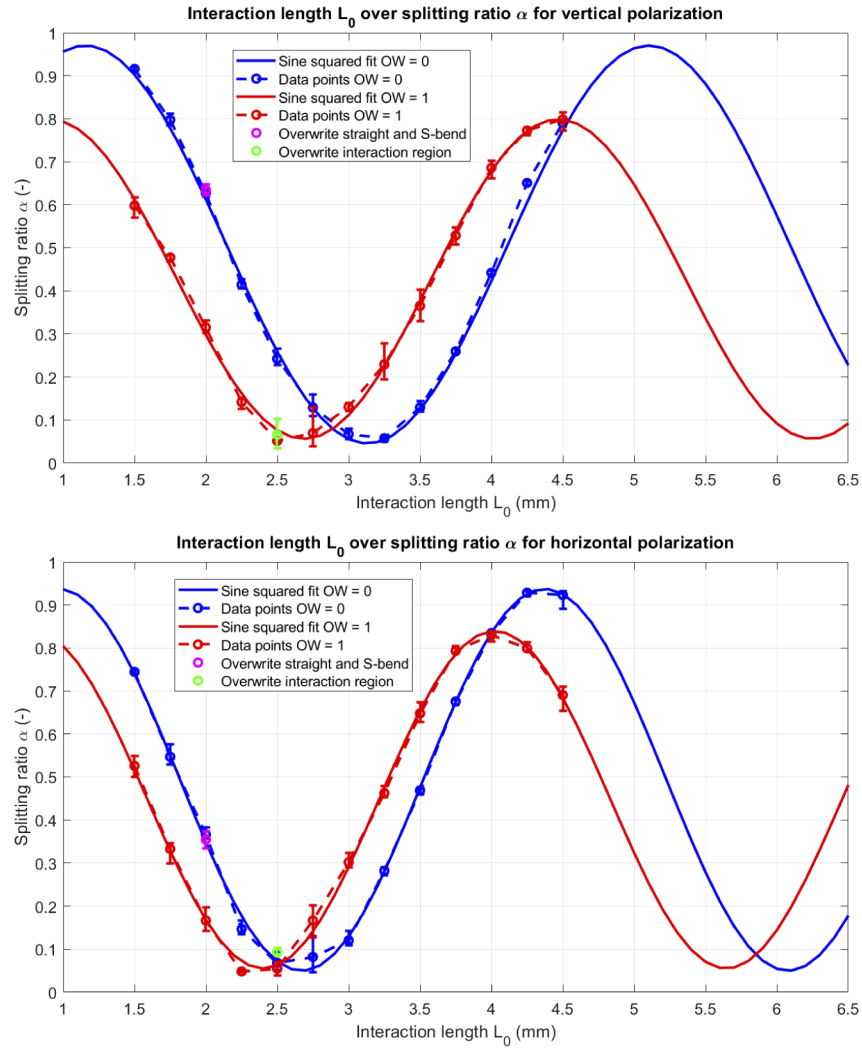
### 3.2. Overwriting directional coupler

Figure 5 shows measurements of the splitting ratio from a range of fabricated DCs. All of the DCs were written in one glass sample with a scanning speed of  $v_w = 17.5$  mm/s and varying interaction lengths from  $L_0 = 1.50$  mm to  $L_0 = 4.50$  mm to probe the sinusoidal response of the splitting ratio. To investigate the impact of overwriting on the splitting ratio, two equivalent set of DCs were written, with a single overwrite pass applied to one. Additionally, DCs were fabricated with one overwriting pass over the interaction region of waveguide 2 at  $L_0 = 2.5$  mm and one overwriting pass over the straight and S-bend regions of waveguide 2 at  $L_0 = 2.0$  mm to investigate the influence of overwriting of different sections. For the overwrite, the same scanning speed and laser parameters were used.

The measured splitting ratios in Fig. 5 for both overwriting and no overwriting DCs follow a clear sine-squared dependency with interaction length  $L_0$  and hence are in good agreement with the coupled mode theory of Section 2. There is a slight difference in the splitting ratio for horizontal and vertical polarization, as commonly observed in previous studies [17]. A decrease in the amplitude  $\sigma^2$  of the sine-squared fit from near unity ( $\sigma^2 = 0.954$  for vertical polarization,  $\sigma^2 = 0.887$  for horizontal polarization) to fractional values ( $\sigma^2 = 0.743$  for vertical polarization,  $\sigma^2 = 0.784$  for horizontal polarization) could be observed after a single overwrite pass.

Figure 5 demonstrates the principle that the splitting ratio of a DC can be adjusted through just a single overwrite by approximately  $\pm 0.3$ , dependent upon the chosen interaction length. The sinusoidal curves are clearly shifted towards lower interaction lengths after overwriting. This occurs to different degrees for incident light with different polarization directions. This effect





**Fig. 5.** Splitting ratio for different interaction lengths ( $L_0 = 1.5$  mm to  $L_0 = 4.5$  mm) for measured data points and the corresponding sine-squared fit for no overwriting ( $OW = 0$ ) (blue) and with overwriting of the entire lower waveguide with  $v_w = 17.5$  mm/s ( $OW = 1$ ) (red) for horizontally (below) and vertically (above) polarized coupled light. The green data point corresponds to one overwriting pass over the interaction region of waveguide 2 with  $v_w = 17.5$  mm/s at  $L_0 = 2.5$  mm. The pink data point corresponds to one overwriting pass over the straight and S-bend regions of waveguide 2 with  $v_w = 17.5$  mm/s for  $L_0 = 2.0$  mm.

can be attributed to birefringence of the guides and shows the need of controlling the ellipticity of the waveguide structure for a polarization-insensitive change of splitting ratio.

The overwriting of the entire interaction region results in a splitting ratio that is similar to the splitting ratio of overwriting the entire waveguide for the same geometry for both horizontal and vertical polarized light (green data point). Furthermore, the overwriting of the straight and S-bend region results in a splitting ratio closely matching the splitting ratio for no overwriting for the same geometry for both polarisations (magenta data point). These findings show that a change of the propagation constant in the straight and S-bend part does not contribute to the major change in splitting ratio in the chosen geometry. The proximity of the splitting ratio between

the parameter for overwriting the entire waveguide and overwriting the interaction region shows that the interaction region contributes the major part for the change in the splitting ratio. These experimental results validate the observations made through simulation.

#### 4. Summary

In this report, simulations and experimental work were performed to assess the influence of overwriting on the splitting ratio of directional couplers. It was shown that by overwriting existing waveguides, the optical properties of a waveguide can be changed, so that a phase mismatch can be induced to change the splitting ratio of a DC. It was found that the optical properties were dependent mainly upon the net fluence. The ellipticity of the waveguides could be maintained at a level near unity over a wide range of net fluence. Consequently, this enabled a proof-of-principle demonstration that the splitting ratio can be trimmed by overwriting one of the waveguides of a DC. Future work will be undertaken to develop a complete protocol for overwriting waveguides to give deterministic tuning of device properties, allowing for change in the waveguide refractive index profile and propagation loss through overwriting. We expect these findings to be beneficial in the future manufacture of DCs with precise splitting ratios, through a combination of online component-wise device characterization [33] and subsequent trimming.

#### Funding

Engineering and Physical Sciences Research Council (EP/M013243/1, EP/R004803/1); Deutsche Forschungsgemeinschaft (GSC80).

#### Acknowledgments

Many thanks are given to Clemens Roeder and Prof. Michael Schmidt from the Institute of Photonic Technologies in Erlangen, Germany for their support. Also, many thanks to Adrian J. Menssen from the Department of Physics in Oxford for the discussions and support with the measurements with the end-fire rig.

#### Disclosures

The authors declare no conflicts of interest.

#### References

1. M. J. Heck, "Highly integrated optical phased arrays: photonic integrated circuits for optical beam shaping and beam steering," *Nanophotonics* **6**(1), 93–107 (2017).
2. C. L. Goldsmith and B. M. Kanack, "Integrated optical transmitter and receiver," U.S. Patent No. 5,479,539. 26 (1995).
3. R. Kaiser, D. Trommer, H. Heidrich, F. Fidorra, and M. Hamacher, "Heterodyne receiver PICs as the first monolithically integrated tunable receivers for OFDM system applications," *Opt. Quantum Electron.* **28**(5), 565–573 (1996).
4. M. G. Thompson, A. Politi, J. C. Matthews, and J. L. O'Brien, "Integrated waveguide circuits for optical quantum computing," *IET Circuits Devices Syst.* **5**(2), 94–102 (2011).
5. T. Meany, M. Gräfe, R. Heilmann, A. Perez-Leija, S. Gross, M. J. Steel, M. J. Withford, and A. Szameit, "Laser written circuits for quantum photonics," *Laser Photonics Rev.* **9**(4), 363–384 (2015).
6. R. G. Hunsperger, "Integrated optics: theory and technology," Springer (2009).
7. W.-P. Huang, "Coupled-mode theory for optical waveguides: an overview," *J. Opt. Soc. Am. A* **11**(3), 963–983 (1994).
8. K. Minoshima, A. M. Kowalevich, E. P. Ippen, and J. G. Fujimoto, "Fabrication of coupled mode photonic devices in glass by nonlinear femtosecond laser materials processing," *Opt. Express* **10**(15), 645–652 (2002).
9. G. D. Valle, R. Osellame, and P. Laporta, "Micromachining of photonic devices by femtosecond laser pulses," *J. Opt. A: Pure Appl. Opt.* **11**(4), 049801 (2009).
10. K. M. Davis, K. Miura, N. Sugimoto, and K. Hirao, "Writing waveguides in glass with a femtosecond laser," *Opt. Lett.* **21**(21), 1729–1731 (1996).
11. K. Suzuki, V. Sharma, J. G. Fujimoto, E. P. Ippen, and Y. Nasu, "Characterization of symmetric  $3 \times 3$  directional couplers fabricated by direct writing with a femtosecond laser oscillator," *Opt. Express* **14**(6), 2335–2343 (2006).

12. G. Li, K. A. Winick, A. A. Said, M. Dugan, and P. Bado, "Waveguide electro-optic modulator in fused silica fabricated by femtosecond laser direct writing and thermal poling," *Opt. Lett.* **31**(6), 739–741 (2006).
13. T. Meany, D. N. Biggerstaff, M. A. Broome, A. Fedrizzi, M. Delanty, M. Steel, A. Gilchrist, G. D. Marshall, A. G. White, and M. J. Withford, "Engineering integrated photonics for heralded quantum gates," *Sci. Rep.* **6**(1), 25126 (2016).
14. Q. Zhang, M. Li, Y. Chen, X. Ren, R. Osellame, Q. Gong, and Y. Li, "Femtosecond laser direct writing of an integrated path-encoded CNOT quantum gate," *Opt. Mater. Express* **9**(5), 2318–2326 (2019).
15. M. Tillmann, B. Dakic, R. Heilmann, S. Nolte, A. Szameit, and P. Walther, "Experimental boson sampling," *Nat. Photonics* **7**(7), 540–544 (2013).
16. A. Crespi, R. Osellame, R. Ramponi, D. J. Brod, E. F. Galvão, N. Spagnolo, C. Vitelli, E. Maiorino, P. Mataloni, and F. Sciarrino, "Integrated multimode interferometers with arbitrary designs for photonic boson sampling," *Nat. Photonics* **7**(7), 545–549 (2013).
17. G. Corrielli, S. Atzeni, S. Piacentini, I. Pitsios, A. Crespi, and R. Osellame, "Symmetric polarization-insensitive directional couplers fabricated by femtosecond laser writing," *Opt. Express* **26**(12), 15101–15109 (2018).
18. S. M. Eaton, W. Chen, L. Zhang, H. Zhang, R. Iyer, J. Aitchison, and P. Herman, "Telecom-band directional coupler written with femtosecond fiber laser," *IEEE Photonics Technol. Lett.* **18**(20), 2174–2176 (2006).
19. I. Pitsios, F. Samara, G. Corrielli, A. Crespi, and R. Osellame, "Geometrically-controlled polarisation processing in femtosecond-laser-written photonic circuits," *Sci. Rep.* **7**(1), 11342 (2017).
20. Z. Chaboyer, T. Meany, L. Helt, M. J. Withford, and M. Steel, "Tunable quantum interference in a 3D integrated circuit," *Sci. Rep.* **5**(1), 9601 (2015).
21. P. C. Humphreys, B. J. Metcalf, J. B. Spring, M. Moore, P. S. Salter, M. J. Booth, W. S. Kolthammer, and I. A. Walmsley, "Strain-optic active control for quantum integrated photonics," *Opt. Express* **22**(18), 21719–21726 (2014).
22. R. Graf, A. Fernandez, M. Dubov, H. Brueckner, B. Chichkov, and A. Apolonski, "Pearl-chain waveguides written at megahertz repetition rate," *Appl. Phys. B* **87**(1), 21–27 (2007).
23. M. A. Dugan, R. L. Maynard, and A. A. Said, "Index trimming of optical waveguide devices using ultrashort laser pulses for arbitrary control of signal amplitude, phase, and polarization," Google Patents (2003).
24. W.-J. Chen, S. M. Eaton, H. Zhang, and P. R. Herman, "Broadband directional couplers fabricated in bulk glass with high repetition rate femtosecond laser pulses," *Opt. Express* **16**(15), 11470–11480 (2008).
25. N. Bisch, J. Guan, M. J. Booth, and P. S. Salter, "Adaptive optics aberration correction for deep direct laser written waveguides in the heating regime," *Appl. Phys. A* **125**(5), 364 (2019).
26. J. Guan, X. Liu, P. S. Salter, and M. J. Booth, "Hybrid laser written waveguides in fused silica for low loss and polarization independence," *Opt. Express* **25**(5), 4845–4859 (2017).
27. S. Rajesh and Y. Bellouard, "Towards fast femtosecond laser micromachining of fused silica: The effect of deposited energy," *Opt. Express* **18**(20), 21490–21497 (2010).
28. A. J. Menssen, J. Guan, D. Felce, M. J. Booth, and I. A. Walmsley, "A photonic topological mode bound to a vortex," arXiv:1901.04439 (2019).
29. C. B. Schaffer, J. F. García, and E. Mazur, "Bulk heating of transparent materials using a high-repetition-rate femtosecond laser," *Appl. Phys. A* **76**(3), 351–354 (2003).
30. ISO11146-1, "Lasers and laser-related equipment - Test methods for laser beam widths, divergence angles and beam propagation ratios - Part 1: Stigmatic and simple astigmatic beams," International Standard (2005).
31. D. Tan, X. Sun, Q. Wang, P. Zhou, Y. Liao, and J. Qiu, "Fabricating low loss waveguides over a large depth in glass by temperature gradient assisted femtosecond laser writing," *Opt. Lett.* **45**(14), 3941–3944 (2020).
32. M. Ams, G. D. Marshall, and M. J. Withford, "Study of the influence of femtosecond laser polarisation on direct writing of waveguides," *Opt. Express* **14**(26), 13158–13163 (2006).
33. J. Guan, A. J. Menssen, X. Liu, J. Wang, and M. J. Booth, "Component-wise testing of laser-written integrated coupled-mode beam splitters," *Opt. Lett.* **44**(12), 3174–3177 (2019).